

## SIMULATING ACCELERATOR STRUCTURE OPERATION AT HIGH POWER\*

V. Ivanov<sup>#</sup>, C. Adolphsen, N. Folwell, L. Ge, A. Guetz, Z. Li, C.-K. Ng, J. W. Wang, M. Wolf, K. Ko, SLAC, Menlo Park, CA 94025, USA

G. Schussmann, UC Davis, CA 95616, USA

M. Weiner, Harvey Mudd College, Claremont, CA 91711, USA

### Abstract

The important limiting factors in high-gradient accelerator structure operation are dark current capture, RF breakdown and electron multipacting. These processes involve both primary and secondary electron field emission and produce plasma and X-rays. To better understand these phenomena, we have simulated dark current generation and transport in a linac structure and a square-bend waveguide, both high power tested at SLAC. For these simulations, we use the parallel, time-domain, unstructured-grid code Tau3P and the particle tracking module Track3P. In this paper, we present numerical results and their comparison with measurements on energy spectrum of electrons transmitted in a 30-cell structure and of X-rays emitted from the square-bend waveguide.

### INTRODUCTION

The X-Band linac R&D for the NLC focuses on developing high gradient accelerating structures to increase linac efficiency and thereby lower the machine cost. In high power tests however, it was found that RF breakdown and dark current generation have prevented the structures from reaching their design gradients. These limiting factors are complex processes for which theoretical understanding is lacking especially when they occur in complicated 3D geometries. Recent advances in parallel code development made by the Advanced Computations Department (ACD) at SLAC have led to a simulation capability for studying dark current and RF breakdown in realistic structures under experimental conditions. A particle tracking module in 3D - **Track3P** has been developed with complete surface physics included, which is interoperable with fields generated either by the parallel eigensolver **Omega3P** for standing wave structures, or by the time-domain field solver **Tau3P** for traveling wave structures. We present simulation results from **Track3P/Tau3P** to two applications with measured data.

### SIMULATION CODES

#### *Tau3p*

This code is a time-domain parallel solver [1], which solve the Maxwell system

$$\frac{\partial \vec{B}}{\partial t} = -\nabla \times \vec{E},$$

$$\frac{\partial \vec{D}}{\partial t} = \nabla \times \vec{H} - \vec{J}.$$

Here **E** and **H** – electric and magnetic fields, **D** = ε **E**, **B** = μ **H** – induction vectors, ε, μ - permittivity and permeability of the media, **J** – excitation current

The numerical algorithm uses explicit scheme of finite volume integration on unstructured grid.

#### *Track3p*

Particle tracking module [2] uses **E** and **B** fields from Tau3p to push particles using the Boris scheme for the motion equations:

$$\frac{d\vec{p}}{dt} = e(\vec{E} + \frac{1}{c}[\vec{v} \times \vec{B}]), \vec{p} = m\gamma\vec{v}, \gamma = \frac{1}{\sqrt{1-v^2/c^2}}$$

with particle injection given by

$$I(t) = \frac{I_{\max}}{1 + \left( \frac{v_0}{a} \left( t - \frac{\phi_0}{\omega} - iD_t \right) \right)^2}$$

where  $I_{\max}$  – amplitude of the injection current, α - half-width of the bunch, ε and μ - charge and mass of particle, Δτ - repetition period,  $E_i$  - injection energy, χ - speed of light, φ - phase of injection, ω - circular frequency of the fields, τ - number of bunch, and

$$v_0 = \frac{c}{\sqrt{1 + \left( \frac{mc^2}{2|e|E_i} \right)^2}}$$

### SURFACE PHYSICS

Thermal emission is described by the Child-Langmuir law

$$J(\vec{r}, t) = \frac{4}{9} \epsilon_0 \sqrt{\frac{2|e|E^2(\vec{r}, t)}{m d}}$$

where ε<sub>0</sub> – vacuum permittivity, δ - distance from the emitter surface where electric field is evaluated.

Field emission in high-gradient field is described by the Fowler-Nordheim formula

$$J(r, t) = 1.54 \times 10^{\left(-6 + \frac{4.52}{\sqrt{\phi}}\right)} \frac{(\beta E)^2}{\phi} e^{\left(\frac{-6.53 \times 10^9 \phi^{1.5}}{\beta E}\right)}$$

where  $\phi$  - work function,  $\beta$  - field enhancement factor.

The model of secondary emission is characterized by the ratio  $\sigma = I_{\text{secondary}}/I_{\text{primary}} = \delta + \eta + r$ , which is a function of the energy of incident primary particles  $e_{\text{pri}}$ . It includes the following components (Fig.1):

- $\delta$ - true secondary emission (0-50 eV); maximum  $e_m \sim 2-4.5\text{eV}$ ; width  $\Delta e \sim 12-15\text{ eV}$ ;
- $\eta$  -non elastic reflection (50 eV- $e_{\text{pri}}$ );
- $r$  - elastic reflection ( $r = 0.05-0.5$  for metals).

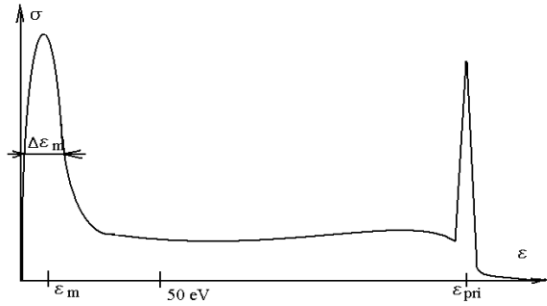


Figure 1: Components of secondary emission.

We use the Lye-Dekker's model [3] for true secondary emission

$$\delta = \frac{\delta_m}{g_m} g\left(z_m \frac{\epsilon}{\epsilon_m}\right), \quad g(z) = z^{-n} \left[1 - e^{-z^{n+1}}\right],$$

where  $\delta_m = 1.4$ ,  $\epsilon_m = 2.5\text{ eV}$ ,  $z_m = 1.84$ ,  $n = 0.35$ .

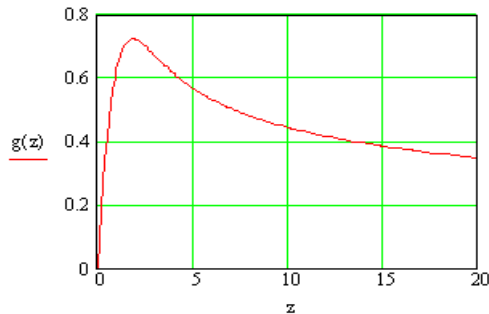


Figure 2. Normalized curve by Lye-Dekker.

### SQUARE BEND SIMULATION

Square bend waveguide (Fig. 3a) used at NLCTA to transport SLED II output power to structures. Electric and magnetic fields are shown at Fig. 3b.

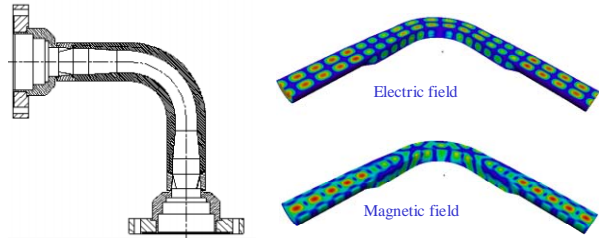


Figure 3. Square Bend Waveguide a) and EM fields b).

High power test on a 90 degree square bend provided measured X-ray data to allow the secondary emission model in **Track3P** be Benchmarked on a simple geometry

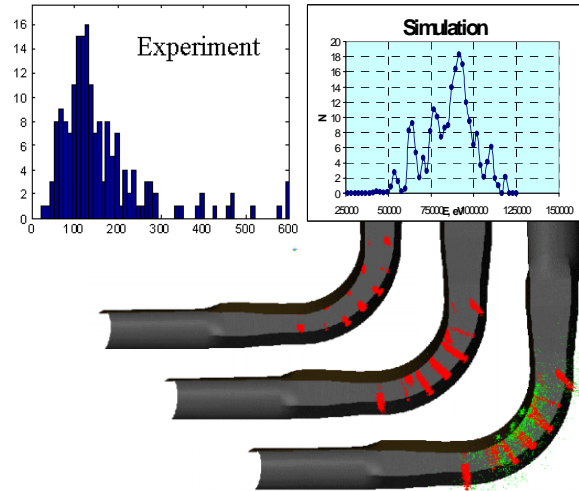


Figure 4. Experimental and numerical data for square bend waveguide. Red colour shows primary particles, green – secondaries.

Good agreement between **Track3P** simulation and measurement indicates high energy X-Rays seen in experiments are due to elastically scattered secondary electrons.

### 30-CELLS HIGH-GRADIENT STRUCTURE

NLC X-band structure showing damage after high power test [2].



Figure 5. Damage in X-band structure.

Realistic simulations needed to understand underlying processes in the structure. Distributed model on a mesh of half million hexahedral elements (Fig.6) for **Tau3P** simulation of field evolution. Field distribution shown at Fig.8, and dark current evolution at Fig.8.

